PAPER

Experimental assessment of impedance-based structural health monitoring in radioactive environment

IOP Publishing Measurement Science and Technology
Meas. Sci. Technol. **34** (2023) 085103 (11pp) https://doi.org/10.1088/1361-6501/accebd

Experimental assessment of impedance-based structural health monitoring in radioactive environment

Fernando de Souza Campos[1], Bruno Albuquerque de Castro[1,*], Helder Tavares de Assis[1], Carlos Alberto Zeituni[2], José Alfredo Covolan Ulson[1] and Fabricio Guimarães Baptista[1]

[1] Department of Electrical Engineering, Sao Paulo State University, Av. Eng. Edmundo Carrijo Coube 14-01, Bauru, SP, Brazil
[2] Radiation Technology Center—CETER, Institute of Nuclear and Energy Center, Av. Prof. Lineu Prestes 2242, São Paulo, SP, Brazil

E-mail: bruno.castro@unesp.br

Received 2 January 2023, revised 10 April 2023
Accepted for publication 20 April 2023
Published 27 April 2023

Abstract

This work presents an experimental study of the influence of radiation on structural health monitoring systems based on the electromechanical impedance method using low-cost piezoelectric diaphragms. For application of the method, the baseline was obtained without radiation and then compared by damage indices after application of radiation. Considering applications in nuclear power plants, the irradiation and calculation of damage indices were performed in the range of 10 kGy–60 kGy at 10 kGy intervals. Impedance measurements were performed in seven frequency bands between 0 and 65 kHz. The results show that, due to the change in the impedance signatures, the damage indices values increase according to the total applied radiation dose, which may indicate a false indication of damage. Besides, results indicate that there are frequency bands less sensitive to radiation and a threshold can be defined to distinguish radiation from structural damage.

Keywords: impedance, piezoelectricity, radiation, SHM, transducer

(Some figures may appear in colour only in the online journal)

1. Introdução

Structural health monitoring (SHM) field have been focusing of research and industry. SHM techniques importance relies on fact that it permits to detect structural damage before a failure occurs guarantying human safety [1, 2]. Moreover, SHM techniques also reduce maintenance costs and has been used in several application fields such as civil engineering, aerospace, and naval industry. There are several SHM techniques proposed in the literature such as eddy currents [3], fiber optic sensors [4], guided waves and infrared thermography [5], Lamb waves [6] and acoustic emission [7]. Among these techniques, the electro-mechanical impedance (EMI) method is one of the most promising SHM technique, because it uses small and light piezoelectric transducers attached to the structure to be monitored, operating simultaneously as an actuator and sensor. These characteristics allow the non-invasive monitoring of different types of engineering structures [8, 9].

The EMI technique relies on an impedance measurement over several frequency ranges. Due to the piezoelectric effect, the electrical impedance of the attached transducer is related to the mechanical impedance of the structure. Therefore, when a failure occurs it changes the mechanical impedance of the structure and, consequently, the electrical impedance of the attached transducer. The damage detection is performed by comparing a reference impedance signature of the healthy structure (also called baseline) with an impedance extracted

* Author to whom any correspondence should be addressed.

from an inspection. In order to quantify the structural condition, two main damage indices are commonly used to perform failure detection and its evolution. These indices are the root-mean-square deviation (RMSD), which is based on the Euclidean norm, and the correlation coefficient deviation metric (CCDM), which is based on the correlation between the two impedance signatures.

Although the EMI technique has been investigated for decades, the effects of some external disturbances such as noise [10] and temperature variations [11] have hindered its application in real structures. In this sense, many researchers have investigated and proposed methods to compensate for the effects of external disturbances, mainly temperature variation, which has been reported as one of the most critical practical problems. Jiang *et al* [10] have proposed a new evaluation index to detect flange bolt looseness under different noise levels. Du *et al* [11] used a multitask convolutional neural network (CNN) for identifying bolts loosening under temperature variation. Recently, Alazzawi *et al* [12] applied the residual learn algorithm to perform damage detection using the time-domain impedance responses. De Rezende *et al* in [13] propose a temperature compensation by a CNN to carry out the correct damage detection. Chowdary and Alapati [14] studied external vibration effects in the EMI technique. A cointegration method to remove temperature effects in the EMI technique was proposed in [15].

In this context, one of the research gaps which was not previously studied is the influence of the radiation, which is present on nuclear facilities, airplanes, satellites, etc [16]. According to a report from of Scientific Committee on the Effects of Atomic Radiation [16] another radiation environment is oil and gas exploration where SHM techniques could be used to monitor metal pipes integrity.

In this scenario, although the EMI technique using piezoelectric sensors has been widely used, the study of the effectiveness of its application in radioactive environments is still incipient and a few studies in the literature have been published focusing on radiation effects only at piezoelectric ceramic transducer itself [17–19]. However, none of these studies presents results of how radiation affects structural damage detection at a structure where the EMI technique is applied. Based on this issue, this work presents the radiation effects on damage detection using the EMI technique and how radiation affects the CCDM and RMSD damage indices. These indexes are the base of damage quantification and, as attested in the previously published mentioned works [10–15], environmental issues such as temperature, vibration, and noise, can alter the damage identification and impair the EMI technique. As radiation can be present in the environment where impedance measurements are taken, it is necessary to investigate the effect of this disturbance in the traditional indexes that are used to quantify damages in the EMI technique.

2. EMI method and radiation effects

2.1. EMI method

Piezoelectric materials have the property of converting mechanical energy into electrical energy by direct piezoelectric effect. Besides, in the reverse effect the electrical energy can produce mechanical energy [20].

The principle of the EMI technique is based on the electromechanical interaction between the mechanical impedance of the structure to be monitored and the electrical impedance of the piezoelectric transducer fastened to the structure due to the reverse and direct piezoelectric effect [21–24]. Figure 1 shows the basic experimental setup for the EMI method, where $Z_E(\omega)$ is the electrical impedance provided by a measurement system.

According to [24], the electrical impedance of the transducer can be determined as:

$$Z_E(\omega) = \frac{1}{j\omega C}\left(1 - \frac{d_{31}^2}{s_{11}^E \varepsilon_{33}^T}\frac{Z_S(\omega)}{Z_S(\omega) + Z_P(\omega)}\right)^{-1} \tag{1}$$

where $Z_E(\omega)$ is the electrical impedance of the transducer at angular frequency ω, C is the static capacitance of the transducer, $Z_P(\omega)$ is the mechanical impedance of the transducer, $Z_S(\omega)$ is the mechanical impedance of the monitored structure, d_{31} is the piezoelectric constant, ${s_{11}}^E$ is the compliance in the constant electric field, ${\varepsilon_{33}}^T$ is the dielectric constant at constant mechanical stress, and j is the complex unit. According to equation (1), any variation in the mechanical impedance Z_P of the structure, caused by some damage, such as cracks and corrosion, implies a corresponding variation in the EMI Z_E.

Therefore, structural damage can be detected by measuring and analyzing the electrical impedance of the transducer. A reference impedance signature is extracted when the structure is in its healthy state and damage can be detected by the electrical impedance variations. Due to SHM field is frequently applied to environment that may have radiation such as petroleum platform, aerospace, etc, it is important to assess EMI technique under this condition. In this sense, the most used damage indices to quantify damage in EMI are the CCDM and RMSD. These indices indicate failure rates by comparing two electrical impedance signatures: an impedance signature used as a reference (baseline) of the intact structure, without damage, and a second impedance signature obtained at monitoring moment of the structure. An index change indicates discrepancies of signatures and thus indicates damage. CCDM and RMSD indices are given, respectively, by [21, 24]:

$$\mathrm{CCDM} = 1 - \frac{\sum_{k=\omega_\mathrm{I}}^{\omega_\mathrm{F}}\left[Z_{E,\mathrm{H}}(k) - \bar{Z}_{E,\mathrm{H}}\right]\left[Z_{E,\mathrm{D}}(k) - \bar{Z}_{E,\mathrm{D}}\right]}{\sqrt{\sum_{k=\omega_\mathrm{I}}^{\omega_\mathrm{F}}\left[Z_{E,\mathrm{H}}(k) - \bar{Z}_{E,\mathrm{H}}\right]^2}\sqrt{\sum_{k=\omega_\mathrm{I}}^{\omega_\mathrm{F}}\left[Z_{E,\mathrm{D}}(k) - \bar{Z}_{E,\mathrm{D}}\right]^2}} \tag{2}$$

and

$$\mathrm{RMSD} = \sum_{k=\omega_\mathrm{I}}^{\omega_\mathrm{F}}\sqrt{\frac{\left[Z_{E,\mathrm{D}}(k) - Z_{E,\mathrm{H}}(k)\right]^2}{Z_{E,\mathrm{H}}^2(k)}} \tag{3}$$

where $Z_{E,\mathrm{H}}(k)$ and $Z_{E,\mathrm{D}}(k)$ are the electrical impedance signatures for the structure under healthy and damaged conditions, respectively, $\bar{Z}_{E,\mathrm{H}}(k)$ and $\bar{Z}_{E,\mathrm{D}}(k)$ are the averaged signatures under healthy and damaged conditions, respectively, and ω_I and ω_F indicate the initial frequency and the final frequency, respectively, of the analyzed frequency band.

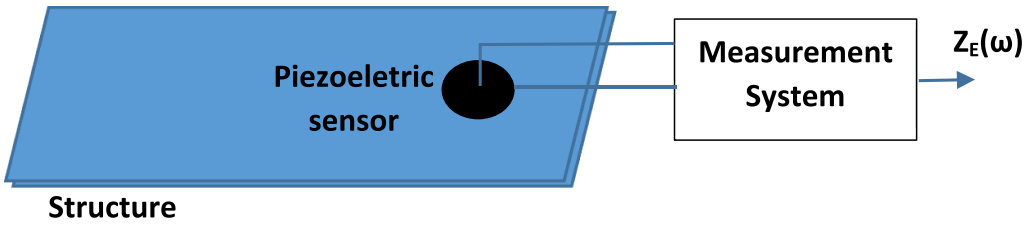

Figure 1. Electromechanical impedance method.

Several other statistical damage indexes have also been proposed in literature such as the mean absolute percentage deviation (MAPD) [25], the time-frequency autoregressive moving average [26], resonant frequencies shift [26], cross-correlation square difference [27]. The goal is to improve the sensibility to perform damage localization, detect the failure severity, or improve the capabilities for measurements under temperature variation, noisy environments etc. For example, MAPD is an index that relates the difference between a given measurement and a baseline curve divided by the baseline. In this sense, MAPD is a cumulative sum of the relative errors between two sequences. Resonant frequencies shift works with the principle that the structural parameter changes cause not only variations in the impedance amplitudes but also the resonance frequency shifts in the impedance curves. Therefore, the frequency shift measurement can be a promising failure detection tool.

It is important to note that the electrical impedance is complex and damage indices can be calculated using the real part, imaginary part, or magnitude of the impedance. In this study, the real part was used to calculate both the CCDM and RMSD indices, since the real part of the impedance has been reported in the literature as being more sensitive to structural damage. Furthermore, the real part is less sensitive to temperature variation than the imaginary part because the dielectric constant ε_{33}^{T} shown in equation (1) is temperature sensitive and it only affects the imaginary part [28].

2.2. Radiation effects

Ionizing radiation can remove electrons from the atom forming ions. According to the frequency of ionizing radiation it is classified into x-ray (10^{17} Hz–10^{19} Hz), gamma radiation (10^{19} Hz–20^{21} Hz) and cosmic radiation ($>10^{21}$ Hz). The sources of this type of radiation are respectively x-ray equipment, radioactive material used in nuclear power plants (gamma radiation) and space (gamma radiation and cosmic rays). The main effects of gamma radiation on piezoelectric transducers are the appearance of internal defects, the change of resonant frequencies and the capacitance of the piezoelectric material [16, 29]. Based on this issue, this article aims to assess the effects of the radiation on the performance of the damage detection based on the EMI technique.

It is important to note that in addition to radiation, other environmental effects such as noise and temperature also cause variations in the impedance signatures. The effects of temperature variation have been reported as one of the most critical problems in the application of the EMI technique [30]. As is well known, temperature variation causes shifts in both frequency and amplitude in the impedance signatures, which can lead to an incorrect diagnosis of the monitored structure [30, 31]. In this study, the experimental tests were carried out under an approximately constant temperature controlled by air conditioning so that the temperature effects can be minimized, allowing to focus the analysis on the radiation effects. Furthermore, as already mentioned, the RMSD and CCDM indices were calculated using the real part of the impedance, which is less sensitive to temperature than the imaginary part [28].

3. Experimental setup

In order to evaluate the radiation effects on the EMI technique, experiments were carried out with an aluminum plate (85 mm × 85 mm × 1 mm). The attached transducers were the 7BB-20-6 piezoelectric diaphragm, manufactured by Murata Electronics North America, Inc. (Smyrna, GA, USA), with a circular brass plate with dimensions 20 mm × 0.2 mm and a circular piezoelectric ceramic with dimensions 14 mm × 0.22 mm. As the thickness of the transducer is very small compared to its diameter, the vibration is predominantly in the radial mode. To simulate damage, two neodymium's magnets, one on the upper side and other on the bottom side, was attached to the host structure. The magnets change the mass of the structure and, consequently, its mechanical impedance $Z_S(\omega)$ indicated in equation (1), simulating structural damage. This procedure has the advantage of not causing permanent damage to the structure. Furthermore, as the applied radiation is cumulative and the objective is to assess how each level of radiation can interfere with the detection of a given structural damage, the addition of magnets allows simulating identical structural damage under different levels of radiation. The impedance of the transducer was measured using a data acquisition device (NI USB-6211) with a sample rate of 250 kHz. A LabVIEW application achieved the impedance calculus according to the circuit presented in [21]. The transducer was excited using a chirp signal with amplitude of 1 V in a frequency range from 0 to 65 kHz with a frequency step of 2 Hz. Figure 2 shows the experimental setup.

Damage detection in the EMI method is based on a damage index that compares the impedance signature of the healthy

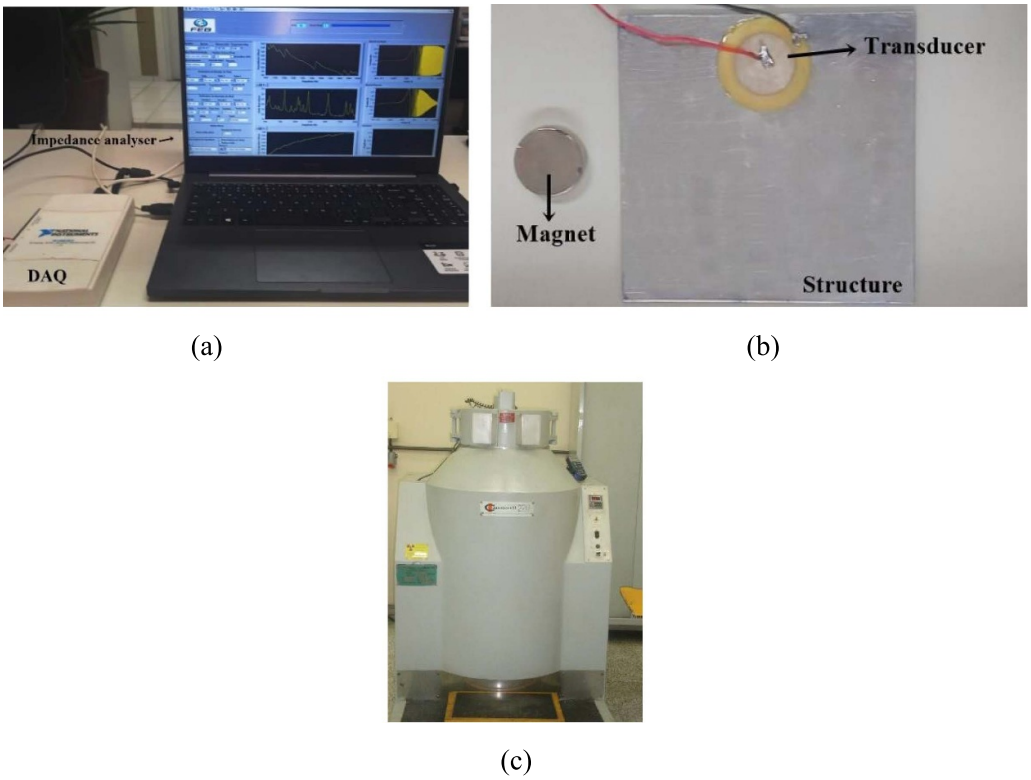

Figure 2. (a) Aluminum plate and neodymium's magnet and (b) notebook with LabVIEW application and DAQ system (c) gamma cell.

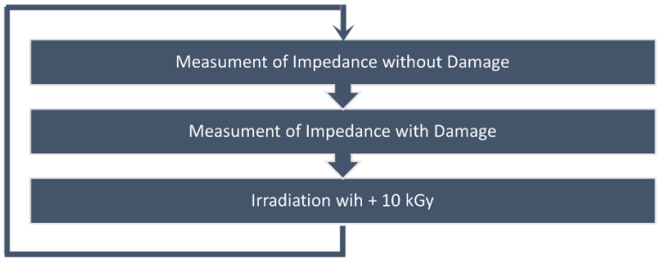

Figure 3. Measurement experimental methodology.

structure (baseline) to the impedance signature of the damaged structure. Thus, initially, the baseline signature was obtained without irradiation and without damage. Afterwards, measurements were carried out with irradiation from 0 kGy to 60 kGy in steps of 10 kGy. The irradiation was done using a gamma cell whose small chamber limited the plate size. Figure 3 summarizes the proposed methodology. The gamma cell (figure 2(c)) permits to set the time of exposure that should be calculated according to the radiation rate of the source, and the total dose desired. According to the radiation rate of the gamma cell, 12 h of irradiation was needed to obtain the total dose of 10 kGy. Therefore, each step lasted 12 h of irradiation to accumulate 10 kGy in each step of the experimental setup. These values are compatible with application of SHM in dry cast storage system, according to [17].

4. Results

4.1. Baseline and indexes without damage under radiation effects

Figure 4 highlights the radiation effects on the real part of the impedance from 2 kHz to 10 kHz. The impedance signature has changed with the dose of radiation since the peaks decrease with the radiation dose. In this context, when the baseline extraction and an undamaged impedance measurement are contaminated with the radiation, these changes reflect in CCDM and RMSD indices as shown in figures 5–11, which assess both indices at seven different frequency ranges of impedance: 2 kHz–10 kHz, 10 kHz–20 kHz, 20 kHz–30 kHz, 30 kHz–40 kHz, 40 kHz–50 kHz, 50 kHz–65 kHz, and 0 kHz–65 kHz, respectively. All indices were calculated using the real part of the impedance.

In general, the indices increase as a function of the radiation. At frequency range from 0 kHz to 10 kHz the CCDM varied from 0.04 to 0.115 (figure 5(a)) and the RMSD from 80 to 120 (figure 5(b)). Therefore, considering percentage change ($\%I$) of the indexes calculated by:

$$\%I = \frac{I_{\mathrm{n}} - I_{\mathrm{p}}}{I_{\mathrm{p}}}.100\%, \tag{4}$$

where I_{n} is the new index value and I_{p} is the past index value, CCDM increased by 187.5% and RMSD by 50% correspondingly to an increase in radiation from 10 kGy to 60 kGy.

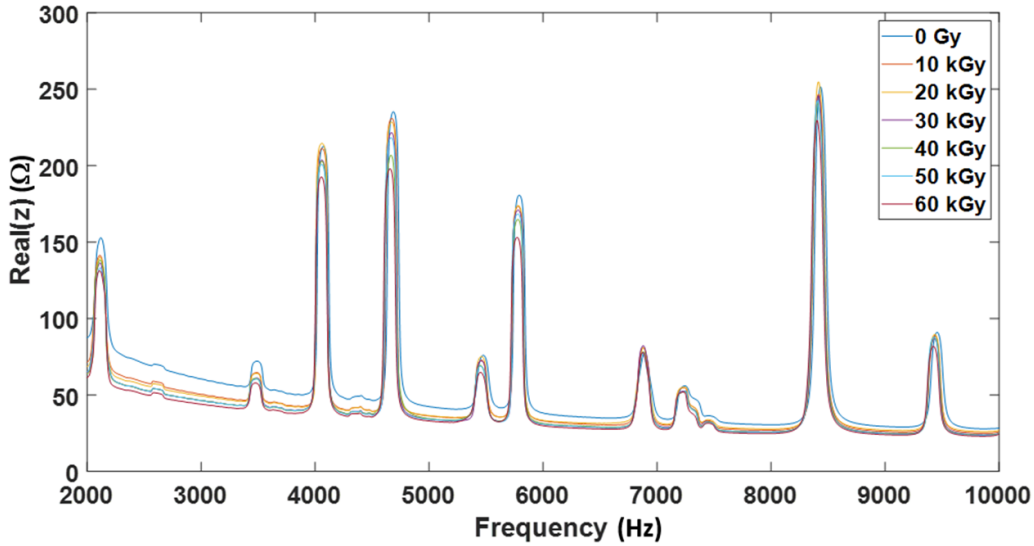

Figure 4. Impedance signature (real part) according to irradiation level.

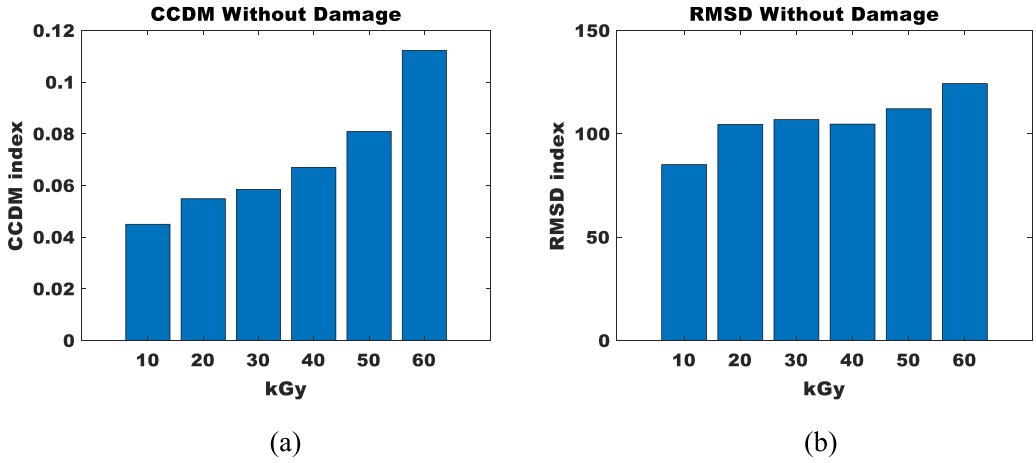

Figure 5. CCDM and RMSD indices without damage at frequency range from 2 kHz to 10 kHz.

Concerning the next frequency range (10 kHz–20 kHz), the CCDM has increased from 0.06 to 0.16 (figure 6(a)) and the RMSD from 90 to 145 (figure 6(b)), which means that the increment of the irradiation dose becomes indexes 167% and 61% more sensitivity to the radiation, respectively. At frequency range from 20 kHz to 30 kHz, the CCDM increased 57.7% from 0.11 to 0.26 (figure 7(a)) and the RMSD 75% from 160 to 280 (figure 7(b)). In the frequency range from 30 kHz to 40 kHz, the CCDM varied from 0.3 to 0.55 (figure 8(a)) and the RMSD from 200 to 260 (figure 8(b)). In this sense, the CCDM has increased by 83% and RMSD by 30%. Regarding the range from 40 kHz to 50 kHz, the CCDM varied from 0.25 to 0.7 (figure 9(a)), which means an increment of 64.2%, and the RMSD varied from about 70 to 120 (figure 9(b)), in other words, an increment of 71.4%. At frequency range from 50 kHz to 65 kHz the CCDM varies from 0.4 to 0.9 (figure 10(a)) and the RMSD varies from 80 to 130 (figure 10(b)). Therefore, CCDM increased by 125% and RMSD by 62.5% correspondingly to an increase in radiation from 10 kGy to the total irradiation of 60 kGy. For the full impedance range (0 kHz–65 kHz), the CCDM varied from 0.04 to 0.1 (figure 11(a)) and the RMSD varied from about 290 to 400 (figure 11(b)). These increments were, respectively, 60% and 37.9%.

4.2. CCDM and RMS indices applied to failure analysis

Figures 12–18 show the results of CCDM and RMSD indices obtained under radiation effects and for the structure with and without damage for the previously studied frequency ranges.

In relation to all cases, despite the radiation dose, CCDM and RMSD were effective to perform damage detection since index values were higher than in the undamaged cases. Considering the CCDM and RMSD values of the undamaged condition produced by the worst condition (60 kGy), it can be noted in figure 12 (frequency range from 2 to 10 kHz) that CCDM increased, on average, 6.5 times with the damage. Concerning the RMSD this value was three times higher in relation to the indexes produced by an undamaged inspection under the higher radiation effect. In this case, RMSD

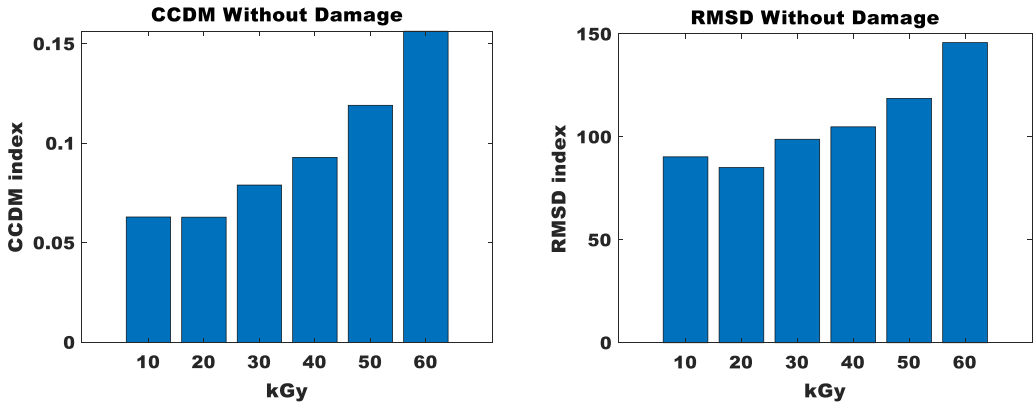

(a) (b)

Figure 6. CCDM and RMSD indices without damage at frequency range from 10 kHz to 20 kHz.

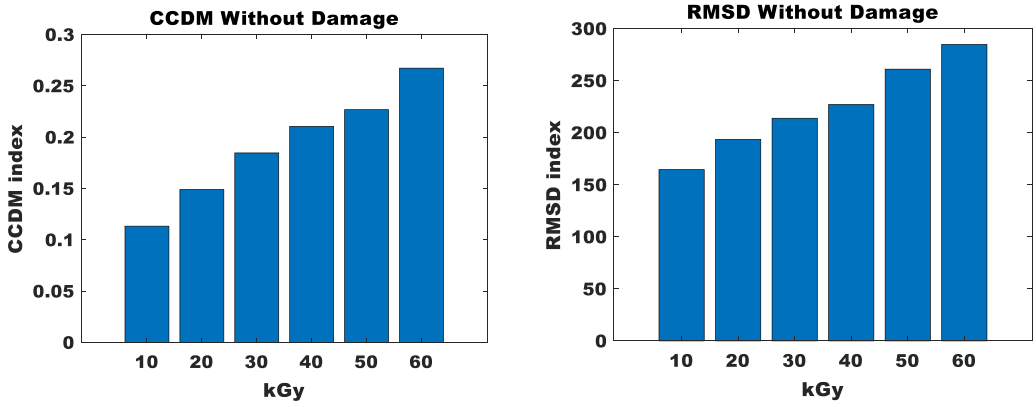

(a) (b)

Figure 7. CCDM and RMSD indices without damage at frequency range from 20 kHz to 30 kHz.

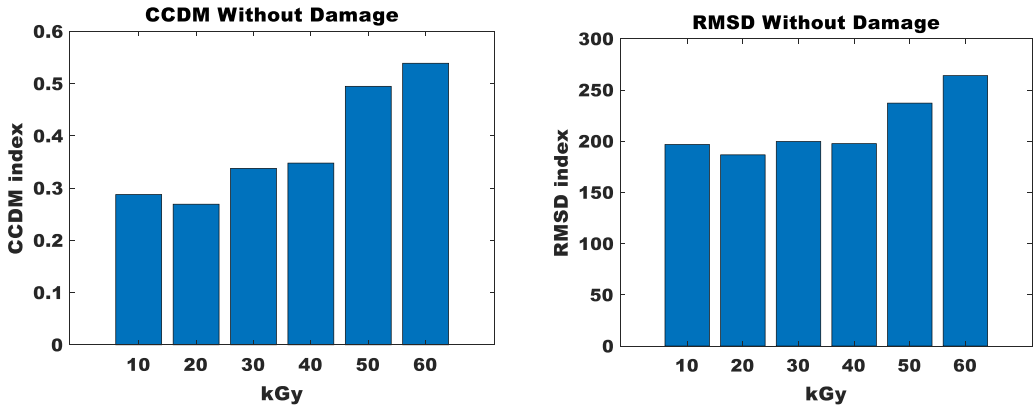

(a) (b)

Figure 8. CCDM and RMSD indices without damage at frequency range from 30 kHz to 40 kHz.

was less sensitive to the damage in relation to CCDM. By achieving the same analysis, these values were, respectively, 337.5% and 189% for CCDM and RMSD considering the range from 10 kHz to 20 kHz (figure 13). For the frequency range from 20 kHz to 30 kHz, CCDM increased by 536% against 78% for the RMSD (figure 14), and for range from 30 kHz to 40 kHz these values were 50% and 54% (figure 15).

Concerning the results presented in the frequency band from 40 kHz to 50 kHz (figure 16), CCDM increased 53%

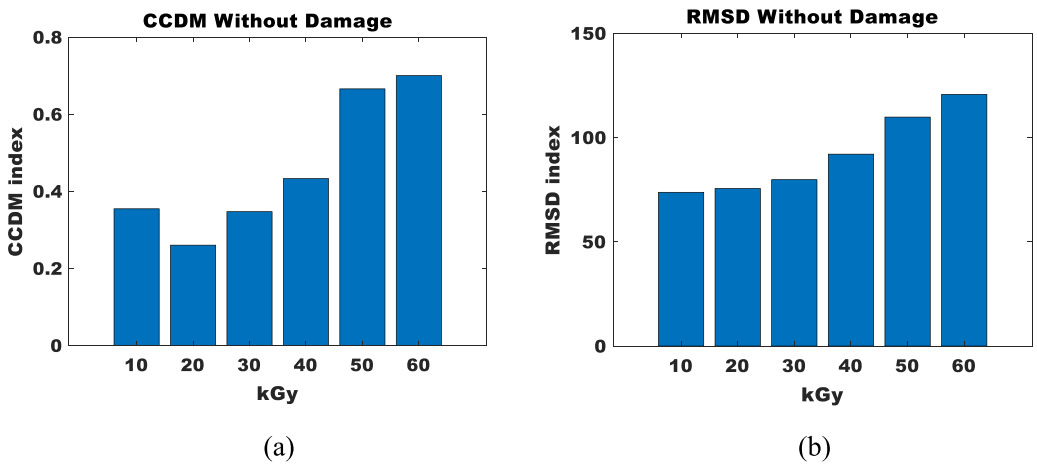

(a) (b)

Figure 9. CCDM and RMSD indices without damage at frequency range from 40 kHz to 50 kHz.

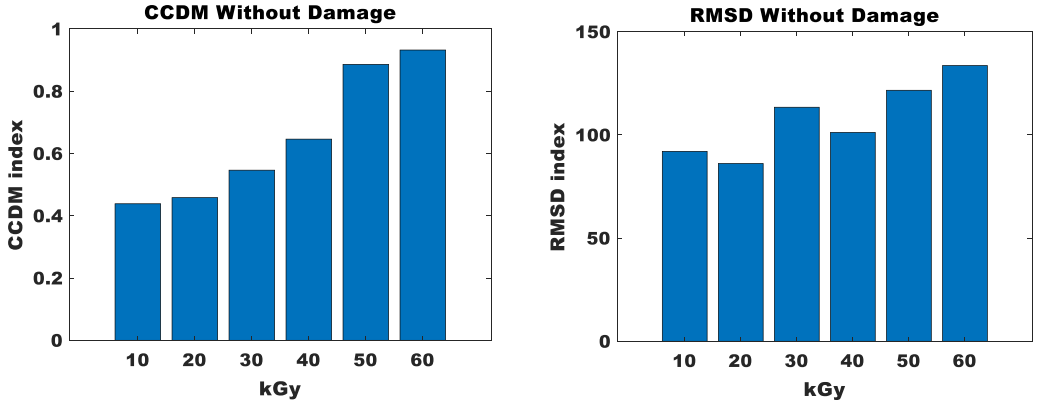

(a) (b)

Figure 10. CCDM and RMSD indices without damage at frequency range from 50 kHz to 65 kHz.

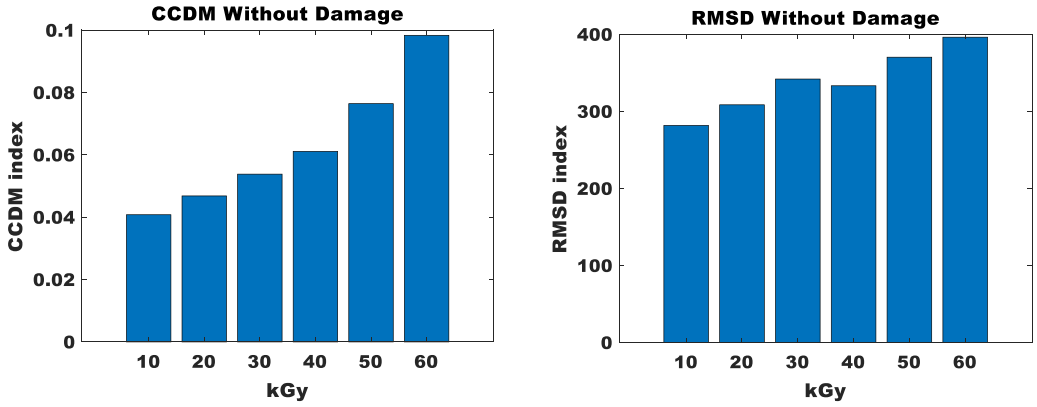

(a) (b)

Figure 11. CCDM and RMSD indices without damage at frequency range from 0 kHz to 65 kHz.

with damage against 300% for RMSD. In relation to the range 50 kHz–65 kHz (figure 17), these values were 42% and 191% for the CCDM and RMSD, respectively. For the full impedance band presented in figure 18, CCDM increased by 300% and RMSD by 150%.

4.3. Discussion

It can be concluded that the radiation may alter the resonant peaks of the impedance signals as observed in figure 4. The impedance variations caused by the radiation effect in the piezoelectric material and in the structure, change the

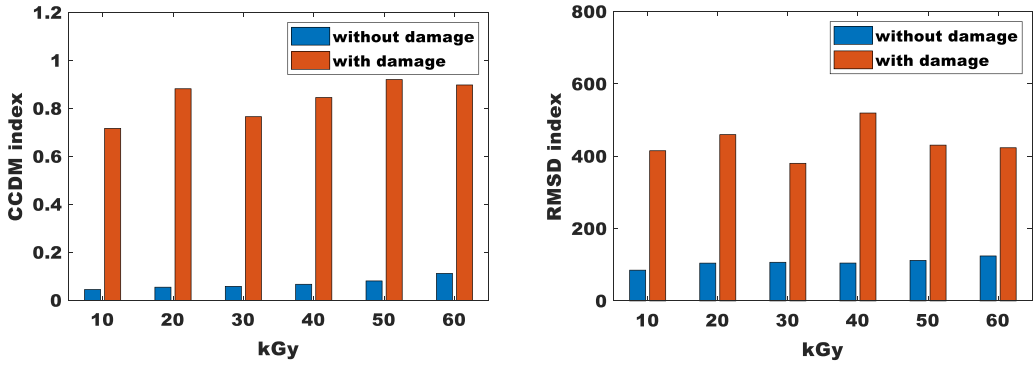

Figure 12. CCDM and RMSD indices at frequency range from 2 kHz to 10 kHz.

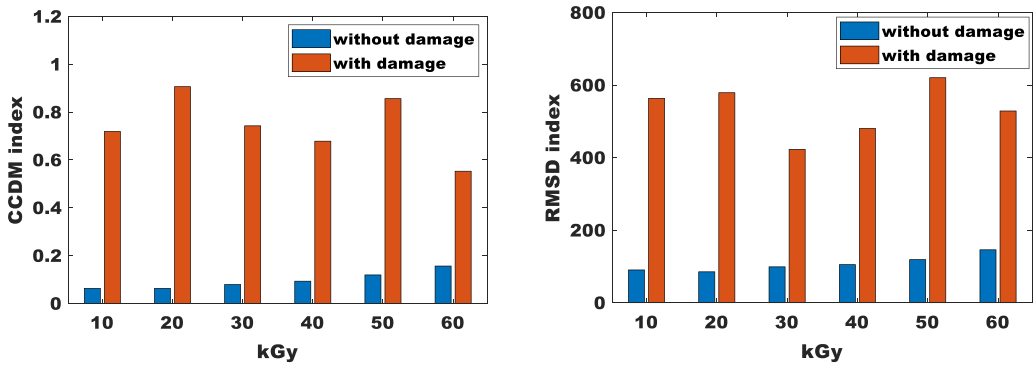

Figure 13. CCDM and RMSD indices at frequency range from 10 kHz to 20 kHz.

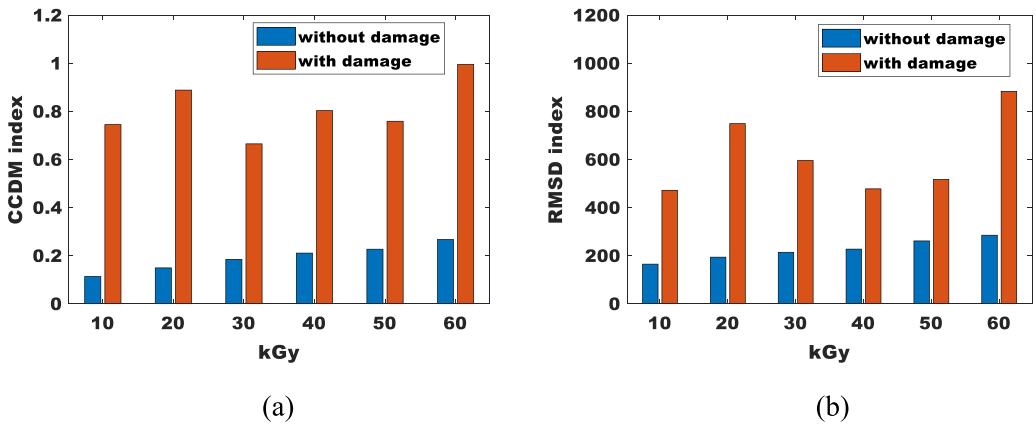

Figure 14. CCDM and RMSD indices at frequency range from 20 kHz to 30 kHz.

impedance curves and, in the case of an undamaged structure, can produce a false diagnosis of damage, since the EMI technique depends on the change of impedance curve to detect damage. For all cases presented in figures 5–11, the indexes reported this behavior since they grow with the dose of radiation applied in the monitored component. However, the CCDM index is more sensitive to impedance variations due to the radiation effect since the growth rate was higher than presented by the RMSD index. By considering the application of the EMI technique under this type of environment like oil and gas exploration, nuclear plants, etc. RMSD index can be a promising alternative to perform damage detection since the index is less sensitive to radiation.

It is also important to note that, according to figure 4, the change in frequency content is influenced by the radiation dose. For example, the radiation effect altered the impedance curves from 2000 Hz to 4000 Hz and impose higher amplitude variation in relation to the band 8000 Hz–10 000 Hz. Based

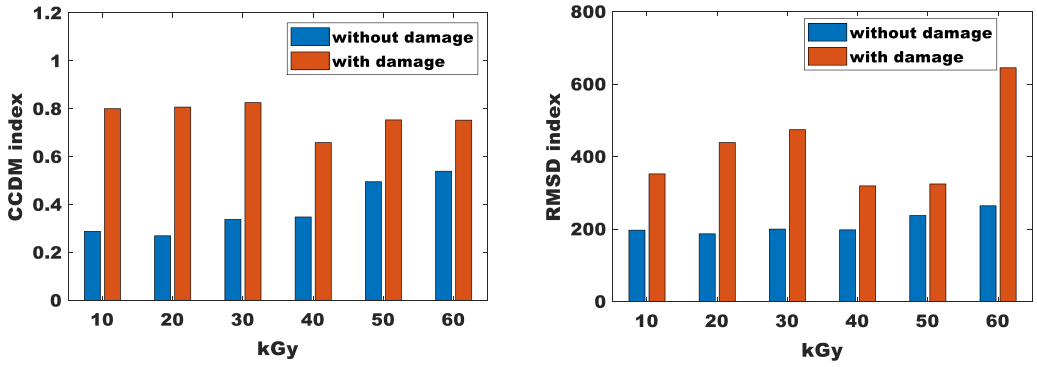

Figure 15. CCDM and RMSD indices at frequency range from 30 kHz to 40 kHz.

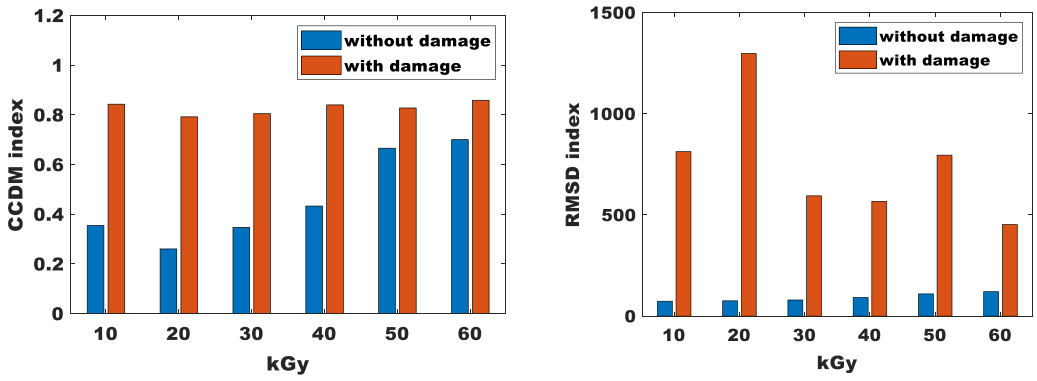

Figure 16. CCDM and RMSD indices at frequency range from 40 kHz to 50 kHz.

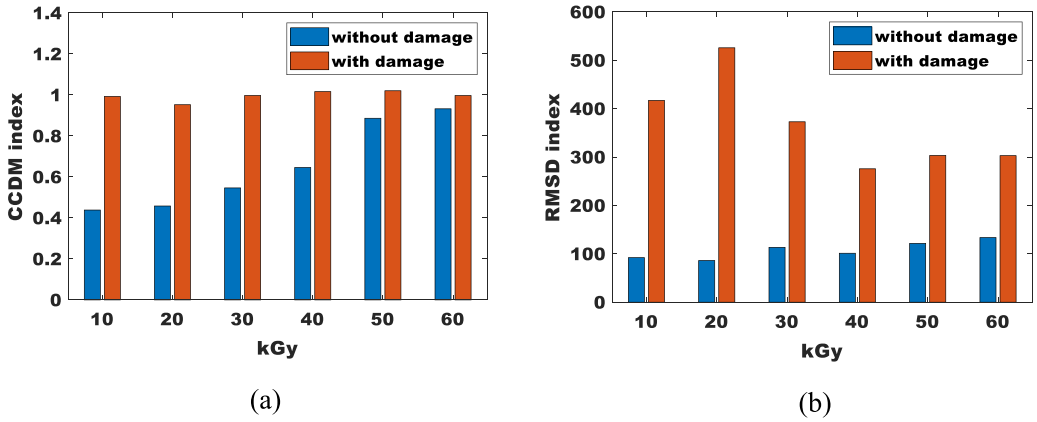

Figure 17. CCDM and RMSD indices at frequency range from 50 kHz to 65 kHz.

on the previously presented results, it can be noted that the RMSD value for the frequency band from 30 kHz to 40 kHz, for undamaged impedance inspection, was less sensitive to the radiation in relation to the other bands.

Concerning the damage analysis, it can be verified the index values were higher than for the damage condition indicating that the EMI technique can work under radiation effect. However, it can be noted that it is necessary to set thresholds from the values of undamaged conditions to perform flaw detection. Considering the RMSD index, which presented lower sensibility for radiation, the highest difference for the undamaged and damaged condition was performed by the impedance extracted between 40 kHz and 50 kHz or the entire spectrum. In both cases, the indexes increased by 300%.

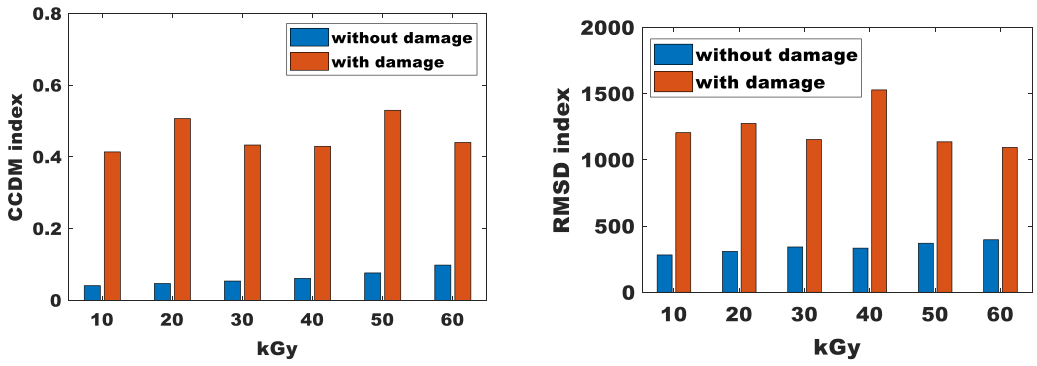

Figure 18. CCDM and RMSD indices at frequency range from 0 to 65 kHz.

5. Conclusions

This article has investigated the effects of radiation on the detection of structural damage based on the EMI method. This analysis is important since in real applications such as nuclear power plants and aerospace structures, the radiation is present and can impair the impedance signatures as this article shows. In this context, CCDM and RMSD were extracted in order to assess the behavior of the traditional damage indices concerning damage detection. Based on the results, it can be concluded that the RMSD is less sensitive to radiation and damage detection, since it presented lower values, as opposed CCDM index which increased at higher rates in relation to RMSD. In addition, frequencies between 30 kHz and 50 kHz were less sensitive to damage for both indices. For future works, other levels of radiation can be studied. Besides, further analysis can discuss how the EMI technique works when the size of the damage increases under radiation effects or other types of noise can impair the impedance measurements.

Data availability statement

The data cannot be made publicly available upon publication because the cost of preparing, depositing and hosting the data would be prohibitive within the terms of this research project. The data that support the findings of this study are available upon reasonable request from the authors.

ORCID iDs

Fernando de Souza Campos https://orcid.org/0000-0002-4458-7750
Bruno Albuquerque de Castro https://orcid.org/0000-0003-4581-1459
Fabricio Guimarães Baptista https://orcid.org/0000-0002-1200-4354

References

[1] Kralovec C and Schargerl M 2020 Review of structural health monitoring methods regarding a multi-sensor approach for damage assessment of metal a composite structures *Sensors* **20** 826
[2] Moll J, Schmidt M, Kasgen J, Mehldau J, Bucker M and Haupt F 2020 Detection of pin failure in carbon fiber composites using the electro-mechanical impedance method *Sensors* **20** 3732
[3] Barrancos A, Silvestre A and Rosado L 2021 Designing a eddy current testing structural health monitoring system *Proc. IEEE Telecoms Conf.* (*Leira, Portugal*) (https://doi.org/10.1109/ConfTELE50222.2021.9435460)
[4] Wu T, Liu G, Fu S and Xing F 2020 Recent progress of fiber-optic sensors for structural health monitoring of civil structure *Sensors* **20** 4517
[5] Balasubramaniam K, Sikdar S, Ziaja D, Jurek M, Soman R and Malinowski P 2023 A global-local damage localization and quantification approach in composite structures using ultrasonic guided waves and active infrared thermography *Smart Mater. Struct.* **32** 035016
[6] Gorgin R, Luo Y and Wu Z 2020 Environmental and operation conditions effects on Lamb waves based structural health monitoring systems: a review *Ultrasonics* **105** 1–15
[7] Cheng C, Liu S and Zhang Y 2021 Robust and low-complexity time-reversal subspace decomposition methods for acoustic emission imaging and localization *IEEE Sens. J.* **21** 3486–96
[8] Tenreiro A, Lopes A and Da Silva L 2022 A review of structural health monitoring of bonded structures using electromechanical impedance spectroscopy *Struct. Health Monit.* **21** 228–49
[9] Cao P, Zhang S, Wang Z and Zhou K 2023 Damage identification using piezoelectric electromechanical impedance: a brief review from a numerical framework perspective *Structures* **50** 1906–21
[10] Jiang X, Zhang X and Yuxiang Z 2020 Evaluation of characterization indexes and minor looseness identification of flange bolt under noise influence *IEEE Access* **8** 157691–702
[11] Du F, Wu S, Xu C, Yang Z and Su Z 2023 Electromechanical impedance temperature compensation and bolt loosening monitoring based on modified unet and multitask learning *IEEE Sens. J.* **23** 4556–67
[12] Alazzawi O and Wang D 2020 Damage identification using PZT impedance signal and residual algorithmic *J. Civ. Struct. Health Monit.* **11** 1225–38

[13] De Rezende S, Moura Junior J, Finzi Neto R, Gallo C and Steffen Junior V 2020 Convolutional neural network and impedance-based SHM applied to damage detection *Eng. Res. Express* **2** 035031

[14] Chowdary D and Alapati M 2021 Effect of external vibrations on electro-mechanical impedance signatures in damage detection *Mater. Today: Proc.* **45** 3398–403

[15] Li X, Qu W, Xiao L and Lu Y 2019 Removal of temperature effect in impedance-based damage detection using the cointegration method *J. Mater. Syst. Struct.* **30** 2189–97

[16] United Nations Scientific Committee on the Effects of Atomic Radiation 2017 Sources, effects and risks of ionizing radiation (Vienna: United Nations Scientific Committee on the Effects of Atomic Radiation (UNSCEAR))

[17] Giurgiutiu V, Postolache C and Tudose M 2016 Radiation, temperature, and vacuum effects on piezoelectric wafer active sensors *Smart Mater. Struct. J.* **25** 035024

[18] Haider F, Mei H, Lin B, Yu L, Giurgiutiu V, Lamp P and Verst C 2018 Piezoelectric wafer active sensors under gamma irradiation exposure toward applications for structural health monitoring of nuclear dry cast storage systems *Proc. SPIE* **10559** 105992F

[19] Lin B, Mendez-Torres A, Gresil M and Giurgiutiu V 2013 Structural health monitoring with piezoelectric wafer active sensors exposed to irradiation effects *Pressure Vessels and Piping Conf.* pp 155–61

[20] Meitzlier H *et al* 1988 IEEE standard on piezoelectricity: an American national standard *IEEE-ANSI 66 Std 176* (*New York*) (https://doi.org/10.1109/IEEESTD.1988.79638)

[21] Baptista F and Vieira Filho J 2009 A new impedance measurement system for PZT-based structural health monitoring *IEEE Trans. Instrum. Meas.* **58** 3602–8

[22] Visalakshi T, Bhalla S and Grupta A 2018 Monitoring early hydration of reinforced concrete structures using structural parameters identified by piezo sensors via electromechanical impedance technique *Mech. Syst. Signal Process.* **99** 129–41

[23] Albakri M and Tarazaga P 2017 Electromechanical impedance–based damage characterization using spectral element method *J. Intell. Mater. Syst. Struct.* **28** 63–77

[24] Freitas E and Baptista F 2016 Experimental analysis of the feasibility of low-cost piezoelectric diaphragms in impedance-based SHM applications *Sens. Actuators* A **238** 220–8

[25] Ioan U, Tudose M and Enciu D 2018 Qualification of PWAS-based SHM technology for space applications *Structural Health Monitoring from Sensing to Processing* (IntechOpen) p 117 (available at: www.intechopen.com/books/6799)

[26] Fan X, Li J and Hao H 2018 Impedance resonant frequency sensitivity based structural damage identification with sparse regularization: experimental studies *Smart Mater. Struct.* **28** 015003

[27] Castro B, Baptista F and Ciampa F 2020 New imaging algorithm for material damage localisation based on impedance measurements under noise influence *Measurement* **163** 107953

[28] Park G, Sohn H, Farrar C and Inman D 2003 Overview of piezoelectric impedance-based health monitoring and path forward *Shock Vib. Dig.* **35** 451–63

[29] Holbert K, Sankaranarayanan S and McCready S 2005 Response of lead metaniobate acoustic emission sensors to gamma irradiation *IEEE Trans. Nucl. Sci.* **52** 2583–90

[30] Wandowski T, Malinowski P and Ostachowicz W 2017 Temperature and damage influence on electromechanical impedance method used for carbon fibre–reinforced polymer panels *J. Intell. Mater. Syst. Struct.* **28** 782–98

[31] Haydarlar G, Tekkalmaz M and Sofuoğlu M 2022 Structural health monitoring method for *in situ* inspection of landing gears *Materials, Structures and Manufacturing for Aircraft. Sustainable Aviation* ed M Kuşhan, S Gürgen and M Sofuoğlu (Cham: Springer)